Eur Biophys J (2010) 39:1493–1501
DOI 10.1007/s00249-010-0607-x

ORIGINAL PAPER

Effects of hypericin on the structure and aggregation properties of β-amyloid peptides

Emilia Bramanti · Francesco Lenci · Antonella Sgarbossa

Received: 11 December 2009 / Revised: 24 March 2010 / Accepted: 20 April 2010 / Published online: 15 May 2010

Abstract We have determined the secondary structure of 1–40 β-amyloid peptides by Fourier-transform infrared spectroscopy (FTIR) and characterized the peptide photophysical properties before and after self-assembly by using intrinsic tyrosine steady-state and time-resolved fluorescence. All measurements were performed in the presence and absence of hypericin (Hyp), an exogenous natural polycyclic pigment that has been shown to inhibit fibril formation and has also been used as a fluorescent probe. We monitored the time course of the aggregation process measuring 405 nm light diffusion at 90° and used thioflavin T to reveal the presence of fibrils. FTIR quantitative analysis evidenced a prevalent random conformation at $t = 0$ with and without Hyp. Fibrils showed a predominant parallel β-sheet structure and a small percentage of α-helix. The results of fluorescence measurements showed that Hyp does significantly interact with peptides in β-sheet conformation. In conclusion, hypericin does hinder the formation of fibrils, but the percentages of parallel β-sheets were not significantly different from those found in samples not treated with Hyp.

Keywords Alzheimer's disease · β-Amyloid · Fluorescence spectroscopy · FTIR spectroscopy · Hypericin · Secondary structure

E. Bramanti
Laboratory of Instrumental Analytical Chemistry,
Istituto per i Processi Chimico-Fisici, CNR, Italian National Research Council, Via G. Moruzzi 1, 56124 Pisa, Italy

F. Lenci · A. Sgarbossa (✉)
Istituto di Biofisica, CNR, Italian National Research Council,
Unità di Pisa, Via G. Moruzzi 1, 56124 Pisa, Italy
e-mail: antonella.sgarbossa@pi.ibf.cnr.it

Abbreviations

EtOH	Ethanol
A-β	β-Amyloid peptide
Hyp	Hypericin
LS	Light scattering = diffusion at 90° of 405 nm light
Tyr	Tyrosine
ThT	Thioflavine T

Introduction

Amyloid aggregates responsible for neurodegenerative disorders such as Huntington's and Alzheimer's diseases show a fibrillar morphology and a predominantly β-sheet secondary structure (Zerovnik 2002; De Felice et al. 2004; Stefani 2004). Fibril formation is a polymerization process, described by a sigmoid curve, recently suggested to be a three-stage process consisting of protein misfolding, nucleation, and fibril elongation (Lee et al. 2007). In this phenomenon, a key role is played by forces common to all proteins, without any meaningful dependence on the specific peptide sequence, including hydrophobic interactions, backbone hydrogen bonding, and stacking interactions.

The main neurotoxic species would be the soluble oligomers (Talaga 2004; Cleary et al. 2005; Chimon et al. 2007) apparently capable of forming pores, which potentially induce cell dysfunction *via* wrong membrane permeabilization (Lashuel and Lansbury 2006).

Alzheimer's disease (AD) is characterized by the presence of typical amyloid plaques in the extracellular space of the brain that are composed of well-ordered fibrillar aggregates of β-amyloid (A-β) peptides. The A-β peptides of different lengths (39–43 residues) are produced by regulated intramembrane proteolysis of a transmembrane protein, amyloid precursor protein (APP), and possess native structural

disorganization. As they are natively unfolded and unstable, a conformational organization *via* a "partially folded" intermediate takes place during fibrillogenesis.

Peptide-peptide interactions resulting in self-assembly phenomena of A-β peptides yielding fibrils (Uversky and Fink 2004) can be modulated and influenced by small organic molecules (Berg 2003; Nilsson 2009), especially polycyclic compounds, which might also disrupt the molecular architectures of the precursors of fibrils (Waters 2004; Gazit 2005; Walsh et al. 2005; Ehrnhoefer et al. 2008). These molecules could, in fact, interact with the π-electron system of A-β aromatic residues targeting the amyloidogenic core and interfering with fibril assembly, as suggested in the case of polyphenols (Ono et al. 2003; Porat et al. 2006) and/or perturb the hydrophobic forces that maintain the side chains of the polypeptide in close contact, thus having a disrupting effect (Bemporad et al. 2006). Recently, it has been shown that hypericin (Hyp), a natural pigment extracted from *Hypericum perforatum*, widely used as a mild antidepressant, can significantly affect and interfere with the early stages of the polymerization process, playing the role of an effective aggregation inhibitor (Sgarbossa et al. 2008).

To gain deeper insights into the quantitative changes of secondary structure of A-β peptides induced by Hyp and to better understand the nature of the pigment-peptide interaction, we have performed a set of Fourier-transform infrared spectroscopy (FTIR) measurements and of steady-state and time-resolved fluorescence emission measurements in different phases of the aggregation process.

Infrared spectroscopy was one of the earliest experimental methods used to evaluate the secondary structure of polypeptides and proteins (Parker 1983; Bandekar 1992). The amide group of proteins and polypeptides presents characteristic vibrational modes (amide modes) that are sensitive to the protein conformation. Furthermore, vibrations of certain amino-acid side chains have absorption bands in the 1,480–1,350 and 1,190–700 cm^{-1} regions and may give small contributions to the intensity of characteristic protein amide bands (Chirgadze et al. 1975).

Intramolecular or intermolecular aromatic and/or hydrophobic interactions can affect the fluorescence emission spectrum as well as the fluorescence quantum yield and lifetime of the aromatic amino acids. In A-β, the three Phe residues, Phe4, Phe19, and Phe20, are fluorometrically silent because of their low quantum yield (Maji et al. 2005). Tyr at position 10 may constitute a useful intrinsic probe of peptide in the N-terminal region. Also Hyp has fluorescent properties that make this pigment a quite reliable probe for monitoring its interaction with the peptide and providing some hints about conformational rearrangements of the site of binding. Indeed, in aqueous solutions, Hyp molecules give rise to polydispersed nonfluorescent aggregates, but they easily associated with suitable macromolecules, thus becoming highly fluorescent monomers (Sgarbossa and Lenci 2001). Consequently, fluorescence measurements can provide important information on the nature of the interactions of Hyp with the A-β peptides under investigation, as well as on the structure of the peptide at different times.

Materials and methods

Thioflavin T (ThT, T3516) and Hyp (H9252) were purchased from Sigma Aldrich (Milan, Italy) and used without further purification. A-β peptides (1–40) were purchased from Biopeptide (San Diego, CA, USA). One of the common problems encountered in in vitro studies of β-amyloid peptide is the high variability of the initial conditions of the sample: if the preparation procedure starts dissolving the peptides at acid pH (about 2) and then the pH of the solution is brought to physiological values (about 7), the preparation goes through the isoelectric point of the peptide (pI = 5.5), where aggregation and precipitation are very probable. To avoid this inconvenience, we have dissolved our peptides in NaOH 2 mM (pH = 10.5), sonicated for 10 min and lyophilized as suggested by Fezoui et al. (2000). For measurements, the powder was instantly dissolved in 0.1 M NaCl MilliQ water solution (pH = 6.5).

Aggregation of A-β was induced by increasing the temperature to 60°C in the thermostatic cell holder of a Perkin-Elmer 50 LS B spectrofluorimeter, equipped with a magnetic stirrer. To monitor the aggregation process, we followed the usual procedure of setting both the excitation and the emission monochromator at 405 nm and measuring light diffusion at 90° (Stege et al. 1999; Wood et al. 1996) [in what follows the term LS (light scattering) will be used for the sake of simplicity].

In all aggregation studies, A-β concentration was 150 μM in 0.1 M NaCl aqueous solution. To avoid misleading results due to its very poor solubility in 0.1 M NaCl aqueous solution and due to the formation of polydispersed aggregates, Hyp was dissolved in spectroscopic-grade EtOH and added to the peptide sample solution before putting the cuvette into the cell holder. Ethanol percentage relative to 0.1 M NaCl peptide solution was always 1% (vol/vol) both in the presence and in the absence of 10^{-5} M Hyp final concentration. Control measurements were performed to verify that the presence of ethanol does not affect the results. At the beginning and at the end of the LS experiments, 75 μl of peptide solution was sampled at $t = 0$ and 3 h (saturation phase of LS curves) and spread on a BaF_2 window for FTIR analysis. FTIR analysis was performed on peptide films after removing the water by evaporation at 21 ± 1°C.

Fluorescence spectra were measured by means of the same Perkin-Elmer 50 LS B spectrofluorimeter. Fluorescence lifetime measurements were performed using an Edinburgh OB920 Fluorimeter [time resolution from 100 ps to 10 μs, H_2 lamp, using time-correlated single photon counting (TCSPC)]. For measuring Hyp fluorescence lifetimes, the selected excitation and emission wavelengths were 550 and 600 nm, respectively, and 270 and 310 nm for Tyr. For each measurement up to 5,000 counts were acquired. Deconvolutions and fits were performed by means of a FAST software package provided by Edinburgh. Optical absorption spectra were measured with a JASCO 7850 spectrophotometer.

Infrared spectra were recorded by using a Perkin-Elmer Spectrum One FTIR Spectrophotometer, equipped with a TGS detector. For each sample, 32 interferograms were recorded, averaged, and Fourier-transformed to produce a spectrum with a nominal resolution of 4 cm^{-1}. Thirty-two scans were enough to obtain a suitable S/N ratio and to keep a balance of aqueous vapor bands with respect to the background spectrum. The typical vapor band did not appear either in the spectra or in the second derivative.

Spectrum software (Perkin-Elmer) and the peak fitting module of Origin 8.0 (Microcal) were employed to run and process spectra, respectively. Prior to curve processing, a straight baseline passing through the ordinates at 1,800 and 1,480 cm^{-1} was subtracted, and spectra were normalized in the 1,700–1,600 cm^{-1} region. This seemed to be a reasonable choice in order to avoid artefacts in absorptions near limits of the region examined (1,700–1,600 cm^{-1}). Then, the second derivatives of the amide I band of the spectra examined (1,700–1,600 cm^{-1} region) were analyzed to determine the starting data (number and position of Gaussian components) required for the deconvolution procedure. The choice of the amide I band for structural analysis is due to the very low contribution of the amino acid side chain absorptions present in this region (Chirgadze et al. 1975), and to its higher intensity with respect to other amide modes.

On the basis of the infrared assignment of amide components, assuming that the extinction coefficient is the same for all the secondary structures, the secondary structure composition can be obtained from the FTIR spectra. The values for the percentages of the different secondary structures are estimated by expressing the peak area value of the bands assigned to each of these structures as a fraction of the total sum of the peak area of the amide I components (Bramanti and Benedetti 1996).

Results and discussion

It was previously shown that in phosphate buffer the aggregation process of A-β (1–40) peptide is inhibited by the presence of Hyp in the medium. With the aim of investigating the secondary structure of the A-β peptide at the different phases of the aggregation process, FTIR in transmission mode was used. As NaCl solutions have to be used to avoid phosphate interference in FTIR measurements, the aggregation process of A-β (1–40) peptide in NaCl aqueous solution in the absence and in the presence of 10^{-5} M Hyp was followed (Fig. 1b). As shown in Fig. 1b, A-β aggregation also takes place in NaCl aqueous solution, whereas in the A-β + Hyp system the LS value is constant.

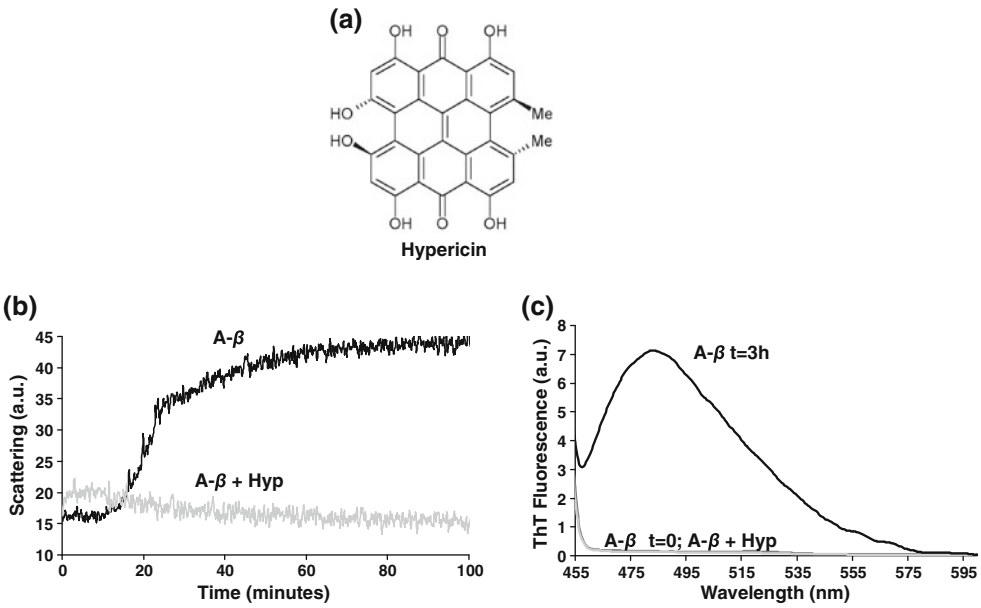

Fig. 1 **a** Hypericin chemical structure. **b** Time-course of the aggregation process at 60°C of 150 μM A-β in 0.1 M NaCl aqueous solution in the presence and in the absence of 10^{-5} M Hyp in 1% EtOH. **c** Fluorescence intensity of ThT (5 μM, λ_{exc} = 442 nm) with A-β at t = 0 and t = 3 h and in the presence of A-β samples in which the fibrillogenesis was inhibited by 10^{-5} M Hyp in 1% EtOH

The presence of A-β fibrils is efficiently revealed by means of ThT, a fluorescent probe, whose fluorescence quantum yield is intrinsically quenched when unbound to amyloid fibrils and increases when bound, because of the blockage of the rotation of the benzothiozole and benzaminic rings with respect to one another (Voropai et al. 2003). At the very beginning of the aggregation process ($t = 0$) for all samples and at $t = 3$ h, when fibril formation is inhibited by Hyp in A-β + Hyp systems, no significant ThT fluorescence signal was detected (Fig. 1b).

It should be noted that A-β is natively unfolded and very unstable and that, whereas at nanomolar concentrations oligomerization and fibril formation do not occur, at micromolar concentrations it is difficult to obtain pure monomers. As stated in the "Material and methods" section, for A-β preparation we followed the Fezoui procedure (Fezoui et al. 2000), which has been demonstrated to produce peptide solutions containing higher yields of monomer and low-order oligomer states (low molecular weight, LMW A-β) and lower concentration levels of pre-existing aggregates or seeds present in the peptide stocks. So, in our experimental conditions, at $t = 0$, a mixture of monomers and oligomers (dimers, trimers, and tetramers) of A-β is probably in equilibrium.

FTIR analysis

The secondary structure of A-β peptide at $t = 0$ and $t = 3$ h was studied in dried films using FTIR in transmission mode. Figure 2 shows the FTIR absorption spectra in the 1,850–1,250 cm^{-1} region of A-β and A-β + Hyp film obtained at $t = 0$ and $t = 3$ h. Spectra reported in Fig. 2 result from averaging FTIR spectra obtained for two different experiments for each condition studied.

The peak at 1,633 cm^{-1} of amide I is associated with a β-structure. The frequency of amide II at 1,546 cm^{-1} is not associated with specific secondary structures. The band at 1,403 cm^{-1} corresponds to the CH_2 bending region. The amide I region was used in this study to investigate quantitative changes in A-β secondary structure by a peak deconvolution approach.

By applying the deconvolution procedure to the amide I region of the FTIR spectra, the percentage of each amide I component was obtained. Table 1 summarizes the quantitative results of the secondary structure of A-β peptides in all conditions studied. Two different peptide films from different solutions were analyzed for all the studied conditions to check the reproducibility of the procedure.

The assignment of the negative peaks displayed by second derivative spectra, corresponding to the frequencies of amide I components obtained after deconvolution, represents a fundamental step in correlating the percentage of the amide I components and the amounts of different secondary structures in the protein.

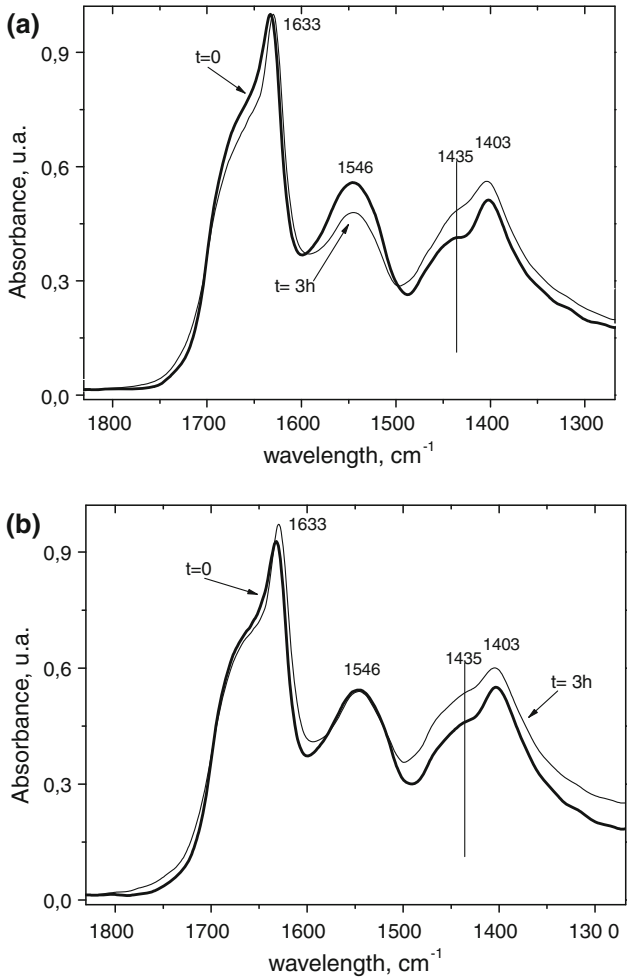

Fig. 2 FTIR absorption spectra in the 1,850–1,250 cm^{-1} region of A-β (**a**) and A-β + Hyp films (**b**) obtained at $t = 0$ (*bold line*) and $t = 3$ h (*thin line*)

It is known that in antiparallel (ap) β-sheet structures, the amide I region displays two typical components, the major one is around 1,630 cm^{-1} and the minor one around 1,695 cm^{-1}. The 1,695/1,630 ratio has been suggested to be proportional to the percentage of antiparallel β-strands in a β-sheet (Krimm and Bandekar 1986; Chirgadze and Nevskaya 1976). Parallel (p) β-sheets show in the amide I region only the major component at 1,630 cm^{-1} (Chirgadze and Nevskaya 1976). The broad component at 1,646–1,648 cm^{-1} is attributed to random chains, and it is characterized by a wide bandwidth. Indeed, in random structures hydrogen bonds are more exposed, and the presence of water molecules as well as adjacent amino acids gives additional strong interactions. These contribute to the distortion of the structures and consequently to an increase in the bandwidth (Veniaminov and Kalnin 1990). The component at 1,676–1,678 cm^{-1} is determined by turns connecting β-strands.

Table 1 Results of the deconvolution procedure applied to the amide I region of the FTIR spectra of A-β peptides with and without 10^{-5} M Hyp at $t = 0$ and $t = 3$ h

Frequency cm^{-1} (bandwidth cm^{-1})	Assignment	Proportion (%)
A-β peptide ($t = 0$)		
1,630 (15)	β-sheets (p + ap)	19
1,648 (40)	Random coil	67
1,678 (20)	β-turns	12
1,691 (10)	β-sheets (ap)	2
A-β peptide ($t = 0$) (replicate)		
1,630 (15)	β-sheets (p + ap)	18
1,646 (37)	Random coil	62
1,676 (22)	β-turns	16
1,690 (11)	β-sheets (ap)	3
A-β peptide + 10^{-5} M Hyp ($t = 0$)		
1,630 (15)	β-sheets (p + ap)	17
1,646 (36)	Random coil	60
1,676 (22)	β-turns	18
1,690 (12)	β-sheets (ap)	4
A-β peptide + 10^{-5} M Hyp ($t = 0$) (replicate)		
1,630 (15)	β-sheets (p + ap)	18
1,646 (41)	Random coil	67
1,676 (20)	β-turns	12
1,690 (11)	β-sheets (ap)	3
A-β peptide ($t = 3$ h)		
1,630 (20)	β-sheets (p + ap)	49
1,650 (16)	α-helix	15
1,669 (24)	β-turns	31
1,688 (14)	β-sheets (ap)	6
A-β peptide ($t = 3$ h) (replicate)		
1,630 (19)	β-sheets (p + ap)	56
1,651 (15)	α-helix	17
1,667 (21)	β-turns	23
1,685 (12)	β-sheets (ap)	4
A-β peptide + 10^{-5} M Hyp ($t = 3$ h)		
1,629 (21)	β-sheets (p + ap)	55
1,653 (18)	α-helix	20
1,672 (19)	β-turns	21
1,687 (11)	β-sheets (ap)	4
A-β peptide + 10^{-5} M Hyp ($t = 3$ h) (replicate)		
1,629 (20)	β-sheets (p + ap)	56
1,653 (15)	α-helix	11
1,672 (21)	β-turns	19
1,687 (12)	β-sheets (ap)	4

p Parallel, *ap* antiparallel, *Hyp* hypericin

A-β amyloid at $t = 0$, treated or not with Hyp, is predominantly composed of a random structure (60–67%) and parallel β-sheets (17–19%) connected by turns (12–18%). A small percentage of antiparallel β-sheet components (2–4%) was also detected.

Fibrils, formed in the absence of Hyp after 3 h, show a significant increase in parallel β-sheets (49–56%) and an increase in β-turns (31–23%), whose components shift from 1,667 to 1,669 cm^{-1} (Surewicz et al. 1993). We also observed a shift in the frequency of antiparallel β-sheet components to 1,685–1,688 cm^{-1}. In both cases a shift toward higher frequencies indicates a more hydrophobic environment.

A component at 1,650–1,651 cm^{-1} in fibrils (15–17%), narrower than the random component (about 15 cm^{-1} vs. 45 cm^{-1} bandwidth), may indicate the formation of α-helix or large loop structures (Krimm and Bandekar 1986; Bandekar and Krimm 1980).

In the presence of Hyp, ThT assay did not reveal the formation of fibrils. However, percentages of β-sheets were not significantly different from those found in samples not treated with Hyp. We observed a significant shift in the band maximum assigned to α-helix and β-turns from 1,650 and 1,669 cm^{-1} in samples not treated with Hyp and to 1,653 and 1,672 cm^{-1} in samples treated with Hyp. This indicates a different spatial distribution and/or state of hydration of these secondary structures and suggests the need for further investigations.

Besides the quantitative difference described above, it is interesting to highlight that a global inspection of the spectra of Fig. 2 shows differences in the amide II/amide I ratio and in the 1,500–1,300 cm^{-1} region. Table 2 shows the ratio of optical densities of amide I and amide II bands (δ1543/δ1633) and of two bands characteristic of CH_2 bending (δ1435/δ1402). In the same table, ThT assay data and β-sheet percentages found by FTIR quantitative analysis are summarized. Amide II/amide I ratio has often been employed to evaluate changes in the secondary structure of proteins during denaturation (Lin and Koenig 1976; Lenk et al. 1989; Kato et al. 1987). This ratio generally increases during denaturation and decreases when peptides again take up an ordered structure.

In our experiments lower values of the δ1543/δ1633 ratio (0.47 and 0.48 in two samples vs. 0.55 ± 0.01, $n = 6$) correlate with the presence of fibrils in the sample, revealed also by LS measurements and by the ThT assay.

Most important, in the presence of Hyp, the value of the amide II/amide I ratio after 3 h was not markedly different (0.54 and 0.55) from the mean value obtained for samples at $t = 0$ (0.56 ± 0.01, $n = 4$), indicating the absence of fibril structures.

Lower values of amide II/amide I ratio were also previously observed in thermal treatment of human serum albumin simultaneously with the formation of inter-chain antiparallel β-sheets (Bramanti and Benedetti 1996).

Table 2 Ratio of optical densities of amide I and amide II bands (δ1543/δ1633) and of two bands characteristic of CH_2 bending (δ1435/δ1402), ThT assay results, and β-sheet percentages

Sample	δ1543/δ1633	δ1435/δ1402	ThT assay	β-sheets, p + ap (%)
A-β (t = 0)	0.54	0.80	–	19 + 2
A-β (t = 0, replicate)	0.56	0.81	–	18 + 3
A-β (t = 3 h)	0.47	0.85	+	49 + 6
A-β (t = 3 h, replicate)	0.48	0.89	+	56 + 4
A-β + Hyp (t = 0)	0.57	0.80	–	17 + 4
A-β + Hyp (t = 0, replicate)	0.56	0.81	–	18 + 3
A-β + Hyp (t = 3 h)	0.56	0.86	–	55 + 4
A-β + Hyp (t = 3 h, replicate)	0.54	0.87	–	56 + 4

ThT Thioflavine T, *p* parallel, *ap* antiparallel, *Hyp* hypericin

The absorptions in the CH_2 bending region (1,500–1,300 cm^{-1}) are affected by changes in peptide structure. Even though CH_2 groups are not usually investigated for conformational studies, their absorptions are affected during β-sheet formation process, as described by Maiti et al. (2006). Indeed, on the basis of the quantitative conformational analysis of A-β reported above, higher values of δ1435/δ1402 ratio in the CH_2 bending region correlate with a high percentage of β-sheet structure, which is observed both in the presence and absence of Hyp. At t = 0, with and without Hyp, δ1435/δ1402 ratio values ranged between 0.80 and 0.81. In fibrils and in samples treated with Hyp after 3 h, this ratio ranged between 0.85 and 0.89.

Thus, the amide II/amide I and δ1435/δ1402 ratios are correlated with the A-β peptide secondary structure and can be considered as simple, qualitative parameters to evaluate the presence of fibrils and β-sheets, respectively, in the A-β samples. In conclusion, FTIR results show that both in the absence and in the presence of Hyp, A-β evolves from random structure (60–66% at t = 0) toward β-sheet structure (49–56%) with a small amount of α-helix (11–20%). In the absence of Hyp, β-sheet oligomers form larger aggregates and fibrils. In the presence of Hyp, β-sheet oligomers are likely stabilized and fibril formation is thus avoided. In addition to the complete conformational analysis of A-β, we defined the amide II/amide I and δ1435/δ1402 ratios, which are correlated with the A-β peptide secondary structure, and can be considered as simple, original, qualitative parameters to evaluate the presence of fibrils and β-sheets, respectively, in the A-β samples.

Fluorescence analysis

With the aim of characterizing the local microenvironment of A-β during self-assembly and the effects of Hyp on it, we performed a steady-state and a time-resolved fluorescence analysis of both Tyr and Hyp.

As shown in Fig. 3a, Tyr fluorescence of A-β slightly decreases with time. This behavior can be explained assuming the occurrence of weak, noncovalent interactions (electrostatic, van der Waals, and solvophobic forces) between the π-electron system of the aromatic residues of the peptide or hydrogen bonds formation with peptide carbonyl groups or with carboxylate side chains of aspartic and glutamic acid (Ross et al. 1992; Cowgil 1976).

When A-β is in the presence of Hyp, a new band around 360 nm is observed (Fig. 3b). This emission band can be attributed to tyrosinate formation (Rayner et al. 1978) and

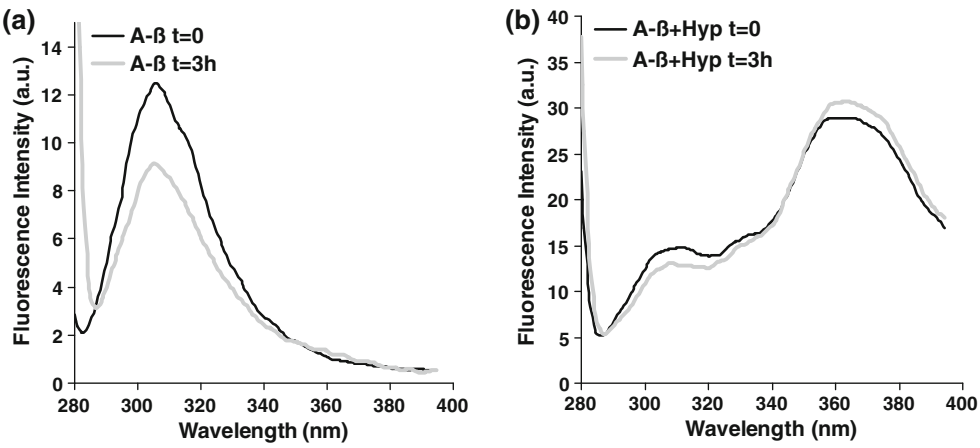

Fig. 3 Fluorescence emission spectra (λ_{exc} = 270 nm) in the Tyr region of A-β at t = 0 and t = 3 h **a** without hypericin (Hyp) and **b** with 10^{-5} M Hyp in 1% EtOH

may be tentatively explained by the occurrence of a nonfluorescent charge transfer complex between Hyp and Tyr, similar to what was reported in the case of Tyr and imidazole (Voicescu et al. 2009). This result seems to indicate that at $t = 0$ Hyp already interacts with the peptide, as suggested also by Hyp fluorescence emission at $t = 0$, and that it is located close to the Tyr position. The 310 and 360 nm emission bands do not vary significantly with time, notwithstanding FTIR results indicating a peptide conformational rearrangement toward a predominant β-sheet structure.

As expected on the basis of a previous study (Sgarbossa et al. 2008), Hyp fluorescence markedly increases with time, reaching a saturation level with an intensity about three times higher than the initial one. This increase in Hyp fluorescence correlates with the increase in the percentage of β-sheet structures with time (Table 1), both of them showing the same increases, around 2.8, after 3 h. As no LS signal increase was observed, it is reasonable to assume that the increase in the β-sheet percentages with time is due to an increase in the number of oligomeric species with β-structure already present at $t = 0$ in our experimental conditions in which a mixture of monomers and oligomers (dimers, trimers, and tetramers) of A-β is in equilibrium. It is also well known that Hyp easily dissolves and becomes fluorescent in hydrophobic environments such as β-sheets.

When dissolved in ethanol, Hyp fluorescence decay can be fitted with a single exponential and a single lifetime is found, about 5.5 ns, $\chi^2 = 0.97$ (Table 3), in agreement with data reported in the literature (Lenci et al. 1995). Adding Hyp to A-β, at $t = 0$ Hyp fluorescence decay can be fitted with a short component, 1.2 ns, 38%, and a long one, 6.1 ns, 62%, with $\chi^2 = 1.003$. Lifetime values and relative percentages do not significantly differ after 3 h, the short component being 1.2 ns, 42%, and the long one, 5.9 ns, 58%, $\chi^2 = 1.038$. The time-independent decay profiles indicate that Hyp associates with A-β with time, always binding to the same molecular pockets. A possible explanation for all of these results is that in our aggregation conditions, over time, many more A-β oligomers are formed that can interact with many more Hyp molecules at the same binding sites (Necula et al. 2007; Lendel et al. 2009, 2010).

Adding Hyp to already formed A-β fibrils, a significantly (39%) shorter component (0.2 vs. 1.2 ns) is revealed together with a 5.5 ns component (61%, $\chi^2 = 1.043$) (Table 3), suggesting that Hyp binding sites of fibrils are different from those of oligomers.

Tyr fluorescence decay can be fitted by a two-exponential curve, regardless of the secondary structure of the peptide, the main difference being the relative percentages of the short- and long-lived components (Table 4). At $t = 0$, when a mixture of monomers and oligomers is in equilibrium, Tyr fluorescence decay shows a minor (12%) short component (1.4 ns) and a major (88%) long component (6.4 ns), with $\chi^2 = 1.002$. The percentages of the two components are not significantly affected by the presence of Hyp: 15 and 85% for the short and long components, respectively ($\chi^2 = 0.93$). Tyr shows two quite similar fluorescence lifetimes after 3 h, both in fibrils [1.4 ns (33%) and 6.1 ns (67%); $\chi^2 = 1.063$] and in the presence of Hyp [1.5 ns (38%) and 6.4 ns (62%); $\chi^2 = 1.28$] (Table 4). With respect to this last point, it is worthwhile noting that Hyp does hinder fibrillogenesis but does not prevent β-structure formation (see FTIR results in Table 2). Lifetime values and relative amplitudes of Tyr are not substantially affected by the presence of Hyp. The increased percentage of the short-lived component in the decay profile after 3 h, both in fibrils and in oligomeric β-structures in the presence of Hyp, matches the hypothesis that Tyr is quite sensitive to the conformational rearrangements toward β-sheets but much less to fibrillar structure. This result is not surprising because it has been demonstrated that, relative to the N-terminal region 1–16 in which Tyr is located, fibrillar and oligomeric A-β differs for a small reduction in local solvent accessibility (Zhang et al. 2009), as also evidenced by the Tyr fluorescence intensity decrease observed by us. The major change in aggregate morphology of oligomers to mature fibrils mainly involves the central hydrophobic core and the C-terminal region.

Table 3 Fluorescence lifetime values and relative amplitudes of 10^{-5} M Hyp ($\lambda_{exc} = 550$ nm, $\lambda_{em} = 600$ nm) in pure EtOH, in the presence of 150 μM A-β at $t = 0$ and $t = 3$ h and added to A-β fibrils

Sample	τ_1 (ns)	A_1 (%)	τ_2 (ns)	A_2 (%)	χ^2
Hyp in EtOh	–	–	5.5	100	0.97
A-β + Hyp ($t = 0$)	1.2	38	6.1	62	1.003
A-β + Hyp ($t = 3$ h)	1.2	42	5.9	58	1.038
A-β fibrils + Hyp	0.2	39	5.5	61	1.043

Table 4 Fluorescence lifetime values and the relative amplitudes of Tyr ($\lambda_{exc} = 270$ nm, $\lambda_{em} = 310$ nm) of 150 μM A-β at $t = 0$ and $t = 3$ h without and with 10^{-5} M Hyp

Sample	τ_1 (ns)	A_1 (%)	τ_2 (ns)	A_2 (%)	χ^2
A-β ($t = 0$)	1.4	12	6.4	88	1.002
A-β ($t = 3$ h)	1.4	33	6.1	67	1.063
A-β + Hyp ($t = 0$)	1.4	15	6.4	85	0.926
A-β + Hyp ($t = 3$ h)	1.5	38	6.4	62	1.274

Concluding remarks

Studies of aggregation of A-β and interactions between small molecules and A-β may constitute important hints for developing inhibitors against Alzheimer's disease. In this study, by means of a combined approach of FTIR and fluorescence techniques, we suggest a model of how the molecule Hyp interacts with A-β. Our experimental results allow us to conclude that Hyp does inhibit fibrillogenesis through interactions with β-sheet portions of A-β peptide oligomers. In the aggregation process, the fraction of A-β oligomers (dimers, trimers, and tetramers) increases and so does the β-sheet percentage, as shown by FTIR results, and, consequently, the number of binding sites for Hyp increases.

This work offers an interesting approach for investigating a variety of analogous systems.

References

Bandekar J (1992) Amide modes and protein conformation. Biochim Biophys Acta 1120:123–143

Bandekar J, Krimm S (1980) Vibrational analysis of peptides, polypeptides, and proteins. VI. Assignment of beta-turn modes in insulin and other proteins. Biopolymers 19:31–36

Bemporad F, Taddei N, Stefani M, Chiti F (2006) Assessing the role of aromatic residues in the amyloid aggregation of human muscle acylphosphatase. Protein Sci 15:862–870

Berg T (2003) Modulation of protein-protein interactions with small organic molecules. Angew Chem Int Ed 42:2462–2481

Bramanti E, Benedetti E (1996) Determination of the secondary structure of isomeric forms of human serum albumin by a particular frequency deconvolution procedure applied to FTIR analysis. Biopolymers 38:639–653

Chimon S, Shaibat MA, Jones CR, Calero DC, Aizezi B, Ishii Y (2007) Evidence of fibril-like beta-sheet structures in a neurotoxic amyloid intermediate of Alzheimer's beta-amyloid. Nat Struct Mol Biol 14:1157–1164

Chirgadze YN, Nevskaya NA (1976) Infrared spectra and resonance interaction of amide-I vibration of the paraellel-chain pleated sheets. Biopolymers 15:607–625

Chirgadze YN, Fedorov OV, Trushina NP (1975) Estimation of amino acid residue side-chain absorption in the infrared spectra of protein solutions in heavy water. Biopolymers 14:679–694

Cleary JP, Walsh DM, Hofmeister J, Shankar MG, Kuskowski M, Selkoe DJ, Ashe KH (2005) Natural oligomers of the amyloid-beta protein specifically disrupt cognitive function. Nature Neurosci 8:79–84

Cowgil RW (1976) In: Chen RF, Edelhoch H (eds) Biochemical fluorescence, Marcel Dekker, New York, pp 441–486

De Felice FG, Vieira MNN, Saraiva LM, Figueroa-Villar JD, Garcia-Abreu J, Liu R, Chang L, Klein WL, Ferreira ST (2004) Targeting neurotoxic species in Alzheimer's disease: inhibitors of Aβ oligomerization. FASEB J 18:1366–1372

Ehrnhoefer DE, Bieschke J, Boeddrich A, Herbst M, Masino L, Lurz R, Engemann S, Pastore A, Wanker EE (2008) EGCG redirects amyloidogenic polypeptides into unstructured, off-pathway oligomers. Nat Struct Mol Biol 15:558–566

Fezoui Y, Hartley DM, Harper JD, Khurana R, Wals DM, Condron MM, Selkoe DJ, Lansbury PT, Fink AL, Teplow DB (2000) An improved method of preparing the amyloid β-protein for fibrillogenesis and neurotoxicity experiments. Amyloid 7:166–178

Gazit E (2005) Mechanism of amyloid fibril self-assembly and inhibition. Model short peptides as a key research tool. FASEB J 272:5971–5978

Kato K, Matsui T, Tanaka S (1987) Quantitative estimation of a-helix content in bovine serum albumin by Fourier transform-infrared spectroscopy. Appl Spectr 41:861–865

Krimm S, Bandekar J (1986) Vibrational spectroscopy and conformation of peptides, polypeptides, and proteins. Adv Protein Chem 38:181–364

Lashuel HA, Lansbury T Jr (2006) Are amyloid diseases caused by protein aggregates that mimic bacterial pore-forming toxins? Q Rev Biophys 39:167–201

Lee C-C, Nayak A, Sethuraman A, Belfort G, McRae GJ (2007) A three-stage kinetic model of amyloid fibrillation. Biophys J 92:3448–3458

Lenci F, Angelini N, Ghetti F, Sgarbossa A, Losi A, Vecli A, Viappiani C, Taroni P, Pifferi A, Cubeddu R (1995) Spectroscopic and photoacoustic studies of hypericin embedded in liposomes as a photoreceptor model. Photochem Photobiol 62:199–204

Lendel C, Bertoncini CW, Cremades N, Waudby CA, Vendruscolo M, Dobson CM, Schenk D, Christodoulou J, Toth G (2009) On the mechanism of nonspecific inhibitors of protein aggregation: dissecting the interactions of R-synuclein with congo red and lacmoid. Biochemistry 48:8322–8334

Lendel C, Bolognesi B, Wahlstroem A, Dobson CM, Astrid Graeslund A (2010) Detergent-like interaction of congo red with the amyloid β peptide. Biochemistry 49:1358–1360

Lenk TJ, Ratner BD, Gendrau RM, Chittur KK (1989) IR spectral changes of bovine serum albumin upon surface adsorption. J Biomed Mater Res 23:549–569

Lin VJC, Koenig JL (1976) Raman studies of bovine serum albumin. Biopolymers 15:203–218

Maiti TK, Ghosh KS, Dasgupta S (2006) Interaction of (-)-epigallocatechin-3-gallate with human serum albumin: fluorescence, Fourier transform infrared, circular dicroism, and docking studies. Proteins 64:355–362

Maji SK, Amsden JJ, Rothschild KJ, Condron MM, Teplow DB (2005) Conformational dynamics of amyloid β-protein assembly probed using intrinsic fluorescence. Biochemistry 44:13365–13376

Necula M, Kayed R, Milton S, Glabe CG (2007) Small molecule inhibitors of aggregation indicate that amyloid-oligomerization and fibrillization pathways are independent and distinct. J Biol Chem 282:10311–10324

Nilsson PKR (2009) Small organic probes as amyloid specific ligands—past and recent molecular scaffolds. FEBS Lett 583:2593–2599

Ono K, Yoshiike Y, Takashima A, Hasegawa K, Naiki H, Yamada M (2003) Potent anti-amyloidogenic and fibril-destabilizing effects of polyphenols in vitro: implications for the prevention and therapeutics of Alzheimer's disease. J Neurochem 87:172–181

Parker FS (1983) Applications of infrared. Raman and resonance raman spectroscopy in biochemistry. Plenum Press, New York

Porat Y, Abramowitz A, Gazit E (2006) Inhibition of amyloid fibril formation by polyphenols: structural similarity and aromatic interactions as a common inhibition mechanism. Chem Biol Drug Des 67:27–37

Rayner DM, Rajcarskain DT, Szabo AG (1978) Excited state acid-base equilibrium of tyrosine. Can J Chem 56:1238–1245

Ross JBA, Laws WR, Rousslang KW, Wyssbrod HR (1992) Tyrosine fluorescence and phosphorescence from proteins and polypeptides. In: Lakowicz JR (ed) Topics in fluorescence spectroscopy. Plenum Press, New York, pp 1–63

Sgarbossa A, Lenci F (2001) Spectroscopic study of visible light effects on hypericin-lens proteins systems. Photochem Photobiol 74:196–200

Sgarbossa A, Buselli D, Lenci F (2008) In vitro perturbation of aggregation processes in beta-amyloid peptides: a spectroscopic study. FEBS Lett 582:3288–3292

Stefani M (2004) Protein misfolding and aggregation: new examples in medicine and biology of the dark side of the protein world. Biochim Biophys Acta 1739:5–25

Stege GJJ, Renkawek K, Overkamp PSG, Verschuure P, van Rijk AF, Reijnen-Aalbers A, Boelens WC, Bosman GJCGM, de Jong WW (1999) The molecular B-crystallin enhances amyloid neurotoxicity. Biochem Biophys Res Commun 262:152–156

Surewicz WK, Mantsch HH, Chapman D (1993) Determination of protein secondary structure by Fourier transform infrared spectroscopy: a critical assessment. Biochemistry 32:389–394

Talaga P (2004) Inhibitors of beta-amyloid aggregation: still an issue of structure and function? Drug Discov Today 1:7–12

Uversky VN, Fink AL (2004) Conformational constraints for amyloid fibrillation: the importance of being unfolded. Biochim Biophys Acta 1698:131–153

Veniaminov SY, Kalnin NN (1990) Quantitative IR spectrophotometry of peptide compounds in water (H_2O) solutions. II. Amide absorption bands of polypeptides and fibrous proteins in α-, β-, and random coil conformations. Biopolymers 30:1259–1271

Voicescu M, El Khoury Y, Martel D, Heinrich M, Hellwig P (2009) Spectroscopic analysis of tyrosine derivatives: on the role of the tyrosine-histidine covalent linkage in cytochrome *c* oxidase. J Phys Chem B 113:13429–13436

Voropai ES, Samtsov MP, Kaplevskii KN, Maskevich AA, Stepuro VI, Povarova OI, Kuznetsova IM, Turoverov KK, Finf AS L, Uverskii VN (2003) Spectral properties of thioflavin T and its complexes with amyloid fibrils. J Appl Spectroscopy 70:868–874

Walsh DM, Townsend M, Podlisny MB, Shankar GM, Fadeeva JV, El Agnaf O, Hartley DM, Selkoe DJ (2005) Certain inhibitors of synthetic amyloid b-peptide (A-B) fibrillogenesis block oligomerization of natural A-β and thereby rescue long-term potentiation. J Neurosci 25:2455–2462

Waters ML (2004) Aromatic interactions in peptides: impact on structure and function. Biopolymers 76:435–445

Wood SJ, MacKenzie L, Maleeff B, Hurle MR, Wetzel R (1996) Selective inhibition of Aβ fibril formation. J Biol Chem 271:4086–4092

Zerovnik E (2002) Amyloid fibril formation. Proposed mechanisms and relevance to conformational disease. Eur J Biochem 269:3362–3371

Zhang A, Qi W, Good TA, Fernandez EJ (2009) Structural differences between Abeta(1–40) intermediate oligomers and fibrils elucidated by proteolytic fragmentation and hydrogen/deuterium exchange. Biophys J 96:1091–1104